# Photoelectron spectroscopy of $OH^-(N_2O)_{n=1-5}$

Joseph B. Kim, Paul G. Wenthold, and W. C. Lineberger
*JILA, University of Colorado and National Institute of Standards and Technology, and Department of Chemistry and Biochemistry, Boulder, Colorado 80309-0440*

(Received 28 August 1997; accepted 10 October 1997)

The 351 nm photoelectron spectra of $OH^-(N_2O)_n$, $n=1-5$, are reported. Each spectrum is composed of a single broad feature that shifts toward higher electron binding energy as the number of solvent molecules increases. Analysis of $OH^-(N_2O)$ spectra at ion temperatures of 200 and 300 K shows that there is significant intensity in the $0_0^0$ transition, and that transitions to the dissociative region of the $OH+N_2O$ potential energy surface are also accessed. The electron affinity of $OH(N_2O)$ is estimated to be $2.14\pm0.02$ eV, from which the $OH-N_2O$ bond dissociation energy is calculated as 0.39 eV. The photoelectron spectra of $OH^-(N_2O)_{n>1}$ are accurately modeled as the convolution of the $OH^-(N_2O)$ spectrum with the $OH^-(N_2O)_{n-1}$. The anion vertical detachment energies and the adiabatic electron affinities for $OH(N_2O)_{n=2-5}$ are obtained and the thresholds for stepwise dissociation of $N_2O$ are located, indicating that photodetachment accesses multiple dissociation channels. © *1998 American Institute of Physics.* [S0021-9606(98)02403-9]

## I. INTRODUCTION

Negative ion photoelectron spectroscopy (PES) is a powerful tool for the study of the energetics of solvation of an ionic chromophore. In previous studies of such cluster anions as $O^-(Ar)_n$ (Ref. 1), $Cl^-(CO_2)$ (Ref. 2), $Br^-(CO_2)_n$ (Ref. 3), $I^-(CO_2)_n$ (Ref. 3), $I^-(N_2O)_n$ (Ref. 3), $I^-(CH_3I)$ (Ref. 4), $NO^-(N_2O)_n$ (Ref. 5), $X^-\cdot(H_2O)_n$ (X=Cl, Br, and I) (Ref. 6), and some distinguishable isomers of $N_2O_2^-$ (Ref. 7), the spectra resembled those of the bare anion, but with each peak in the spectrum broadened and shifted uniformly toward higher electron binding energies (eBE). This shift of the spectrum without modification of the main features implies that the negative charge in the cluster remains largely localized on the initial anion. The shift of the cluster ion photoelectron spectrum is due to the fact that the ion–solvent bond is generally much stronger than the corresponding neutral–solvent bond. The increased width of what was a single vibrational peak in the bare ion photoelectron spectrum arises from unresolved low-frequency van der Waals vibrational modes in the neutral complex excited upon photodetachment. Several studies have also been completed on clusters in which, unlike those listed above, the charge is fairly delocalized, and the spectra bear little resemblance to a single unit within the complex. These studies have been carried out in our laboratory,[8,9] as well as those of Bowen,[10,11] Johnson,[12] Neumark,[13] Smalley,[14,15] Gantefor,[16–18] Meiwesbroer,[19,20] Kaya,[21–23] and Wang,[24–28] and include ions such as $Cu_n^-$ (Refs. 9, 15, and 17), $Ag_n^-$ (Ref. 8), $(H_2O)_n^-$ (Ref. 10), $(CsCl)_n^-$ (Ref. 11), $(CO_2)_n^-$ (Ref. 12), $C_n^-$ (Ref. 13), $Si_n^-$ (Ref. 14), $Ge_n^-$ (Ref. 14), $Fe_n^-$ (Ref. 28), $Cr_n^-$ (Ref. 26), $Ti_n^-$ (Ref. 25), and $V_n^-$ (Ref. 24).

The energetic relationships for addition of a single molecule to a cluster are illustrated in the energy diagram in Fig. 1. The relationship between the adiabatic electron affinities (EA) and the bond energies ($D_0$) of the anion and the neutral can be determined from a simple thermochemical cycle,

$$\mathrm{EA}(A\cdot M_n)=\mathrm{EA}(A\cdot M_{n-1})+D_0(A^-\cdot M_{n-1}-M)-D_0(A\cdot M_{n-1}-M), \quad (1)$$

where $\mathrm{EA}(A\cdot M_n)$ is the adiabatic electron affinity of the neutral core with $n$ solvent molecules, and $D_0(A^-\cdot M_{n-1}-M)$ and $D_0(A\cdot M_{n-1}-M)$ are the bond energies of the anion and neutral, respectively. Because the electrostatic forces responsible for the binding energy in the anionic cluster are much greater than the neutral, the bond dissociation energy in the anionic cluster is sometimes approximated to be the difference in electron affinities of the two clusters, i.e., $D_0(A^-\cdot M_{n-1}-M)\cong\mathrm{EA}(A\cdot M_n)-\mathrm{EA}(A\cdot M_{n-1})$.

For some systems the geometry of the negative ion is significantly different from that of the neutral, and it is not possible to measure the EA spectroscopically. In these cases, poor Franck–Condon factors in the $0_0^0$ transition, combined with activation of many vibrational modes, make it difficult to locate and identify the origin. The most intense peak is instead assigned to a quantity referred to as the vertical detachment energy (VDE). However, the energy obtained for the VDE can correspond to a neutral with a significant amount of vibrational excitation. In addition, it is possible to form the neutral with energies above the dissociation limit. For example, Continetti and co-workers have examined the photoelectron spectra and the photofragment kinetic energy release spectra of $O_4^-$, and have shown dissociative photodetachment occurs when the neutral is formed at energies exceeding the $O_2$–$O_2$ bond energy.[29] Similar effects have been seen in $Cu_2$ photoelectron spectra.[8,9]

Solvated ions can also potentially undergo dissociative photodetachment, because the binding energies between the neutral core and the solvent molecules are very small and there is a large difference in the geometry between the ion and the neutral. In such a case photodetachment leads to formation of the neutral with large amounts of vibrational energy in the weak bond, and may well include dissociation continua. In this paper, we describe our photodetachment studies of the solvated hydroxide ion, $OH^-(N_2O)_{n=1-5}$.

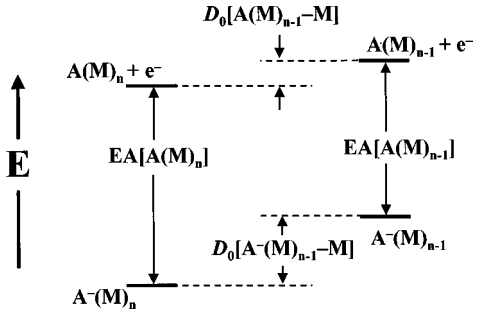


FIG. 1. Schematic diagram illustrating the thermodynamic relationships of the bond dissociation energies in the anionic and neutral clusters. These relationships are applied specifically to derive bond dissociation energies of $OH^-(N_2O)_n$ in the text.

In previous photodetachment studies, hydroxide has been a precursor to forming strongly interacting complexes where the electron is not localized on a single chromophore. In the $H_3O_2^-$ complex, where the bond energy exceeds 1 eV due to hydrogen bonding,[30,31] no barrier exists for proton transfer within the symmetric complex $OH^-$–HOH $\leftrightarrow$HOH–$^-$OH. In addition, hydroxide is one of two charge centers in the $H_3O^-$ complex, where $OH^-(H_2)$ and $H^-(H_2O)$ are possible local minima on the negative-ion potential energy surface. Photoelectron spectroscopy of these systems has provided information on the transition state region of bimolecular hydrogen transfer reactions involving the hydroxyl radical.[32–36] Because of the charge delocalization, the spectrum bears little resemblance to the bare $OH^-$PES.[37]

The reaction of $OH^-$ with $N_2O$ has been examined previously by Bierbaum and co-workers.[38–40] Using a selected ion flow tube, they found that oxygen scrambling occurs in the very slow reaction between isotopically labeled hydroxide and $N_2O$,

$$^{18}OH^- + N_2{}^{16}O \rightarrow {}^{16}OH^- + N_2{}^{18}O. \quad (2)$$

They proposed a mechanism where the hydroxide combines with $N_2O$ to form a long-lived intermediate in which intramolecular proton transfer can occur prior to dissociation. The proposed intermediate in this reaction is a covalently bonded $HONNO^-$ structure. Sheldon[41] has carried out *ab initio* calculations at the MP2 level on the $OH^- + N_2O$ surface and has found that the covalently bonded structure is a local minimum, 0.21 eV more stable than the reactants. The global minimum, however, was determined to be the $OH^-(N_2O)$ ion–molecule complex bound by 0.41 eV.

The equilibrium geometry of $OH^-(N_2O)$ will radically alter upon removal of the excess electron. Nitrous oxide has a small dipole moment ($\mu = 0.1608$D)[42] and a significant quadrupole moment ($\Theta = -3.36\times10^{-26}$ esu cm$^2$),[43] and is best described by $N\equiv\overset{+}{N}-\overset{-}{O}$ with a small contribution from $\overset{-}{N}=\overset{+}{N}=O$. In the anion the central positive charge in $N_2O$ leads to a T-shaped geometry where the oxygen in $OH^-$ bonds electrostatically with the central nitrogen. *Ab initio* calculations at the MP2 level agree with this qualitative prediction of the structure of $OH^-(N_2O)$.

Upon removal of the electron from the complex, the dominant interactions that govern the geometry are the much weaker dispersion and induction van der Waals forces. Although no experimental or computational studies have been reported for $OH(N_2O)$, the structure of this species is expected to be similar to that of $HF(N_2O)$, a system that has been studied in detail. Both computational[44] and experimental studies[45,46] indicate that the terminal charge distribution of $N_2O$ interacts with HF to form two distinct isomers of F-H–NNO and F-H–ONN, corresponding to H–N and H–O van der Waals bonds, respectively. Therefore, the $OH(N_2O)$ complex is expected to have a similar geometry, where the hydrogen bonds to one of the terminal atoms in $N_2O$.[47]

In this paper we examine the photoelectron spectra of $OH^-(N_2O)_{n=1-5}$ to obtain accurate values for the adiabatic electron affinities and the related bond energies. Spectra of $OH^-(N_2O)$ obtained at two different ion temperatures are reported, and comparison of the two spectra indicates that there is significant Franck–Condon intensity in the origin. The paper is organized as follows. In Sec. II we briefly describe the experimental apparatus and technique, including the production of anionic clusters. Spectra are presented in Sec. III, together with vertical detachment energies and photoelectron angular distributions. Section IV A includes Franck–Condon analyses to model the photoelectron spectra of $OH^-(N_2O)$ formed under room-temperature and liquid nitrogen cooled conditions. The adiabatic electron affinity of $OH(N_2O)$ is determined and the OH–$N_2O$ bond dissociation energy is estimated. These values are then used to calculate the bond dissociation energy of the anion. In Sec. IV B the shape of the $OH^-(N_2O)$ spectrum is then used to model the spectra of larger clusters, using the electron affinity as the only free parameter. Dissociative photodetachment thresholds for loss of multiple $N_2O$ are located within the spectral profiles. The values for the electron affinity are then used to calculate the thermodynamic sequential bond dissociation energies for larger clusters in Sec. IV C.

## II. EXPERIMENT

The negative-ion photoelectron spectrometer used in this experiment has been described in detail[48] and only a brief description is provided here. The ion beam apparatus consists of three major components: a thermal energy ion molecule reactor ion source, a mass filter, and the laser interaction and electron energy analysis region.

Negative ions are produced in a flowing afterglow source[48] equipped with a liquid nitrogen cooled jacket. The ions are entrained in a flow of approximately 0.5 Torr of He and gently extracted from the flowing afterglow through a 1 mm aperture on a nosecone. They then enter into a differentially pumped region where they are accelerated to 700 eV, focused, and mass-selected using a Wien velocity filter. The mass-selected ions are then decelerated to 40 eV and injected into the laser interaction region where they intersect a $\sim$100 W 351.1 nm laser beam inside a high finesse buildup cavity.[49] The laser polarization can be rotated from magic angle (54.7°), to parallel (0°) and perpendicular (90°), to the

electron collection direction, in order to carry out angular distribution studies. A small solid angle of photoelectrons is collected and energy analyzed by a hemispherical analyzer with a resolution of about 8 meV, and detected using a position-sensitive microchannel plate detector. The photoelectron spectra are converted to one with an absolute center-of-mass kinetic energy by scaling relative to a reference spectrum that has a well-known electron affinity. The photoelectron spectrum of $O^-$ is used in this study as the reference.[50] The spectrum of $O^-$ was recorded at the beginning and end of each data session and the drift in the spectrum due to contact potentials was found to be less than 1 meV.

Hydroxide ions are produced in a microwave discharge cavity on a mixture of $N_2O$ and $CH_4$. Solvated hydroxide ions are formed by association reactions with a few percent trace amount of $N_2O$ added through a ring inlet located downstream from the $OH^-$ formation region. At room temperature, only $OH^-(N_2O)$ ions are formed in abundance (approximately 50 pA), larger clusters are formed only in trace amounts ($<10$ pA). Cooling the flowing afterglow with liquid nitrogen enhances the formation of larger clusters. When cooled, ion currents of $>50$ pA are produced for ions as large as $OH^-(N_2O)_6$. The ion vibrational temperature is estimated to be 200 K for ions produced under liquid nitrogen cooled conditions, and 300 K for ions produced with a room-temperature flow tube. These estimates are on the basis of measured hot band intensities in systems[51] that have been studied previously.

## III. RESULTS

The extra electron in $OH^-$ adds to a nonbonding $2p\pi$-orbital with a very small geometry difference between the anion and the neutral.[52,53] As a consequence, only $\Delta v = 0$ transitions are observed, and the photoelectron spectrum is comprised of a single 30 meV width vibrational feature with an adiabatic electron affinity of 1.827 664(4) eV. This accurate electron affinity arises from threshold photodetachment studies[52–54] of $OH^-$. In addition, high-resolution photoelectron spectra of $OH^-$ have been obtained by Hotop.[37] The photoelectron spectrum shows resolved transitions to both spin-orbit states[55] of hydroxyl radical and also exhibits partially resolved $P$, $Q$, and $R$ rotational branches. The photoelectron angular distributions and the lack of a vibrational progression confirm the location of the extra electron in a nonbonding $p\pi$-orbital. Detailed analyses of both the photoelectron spectra[37] and the threshold photodetachment spectra[52,53] are available elsewhere. The present photoelectron spectrum of $OH^-$ is completely consistent with these earlier studies.

The structure of $OH^-$ should not change significantly upon addition of $N_2O$ solvent molecules, with the consequent expectation that the photoelectron spectrum of $OH^-$ $(N_2O)$ should also consist of a single peak corresponding to $\Delta v = 0$ in $OH^-$, shifted to higher electron binding energy by the presence of the solvent molecule and with the peak broadened as a result of excitation of low-frequency van der Waals

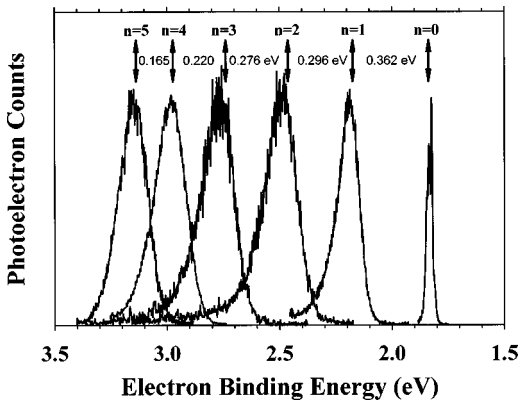


FIG. 2. The 351 nm (3.531 eV) photoelectron spectra of $OH^-(N_2O)_n$, $n=0-5$.

modes in the neutral $OH(N_2O)$ photoproduct (Fig. 1). Qualitatively, such a feature was observed in the photoelectron spectra of $OH^-$ with one through five $N_2O$ solvent molecules. The 351.1 nm photoelectron spectra of all six of these species are shown in Fig. 2. All of these spectra were obtained under conditions in which the flowing afterglow ion source was cooled with liquid nitrogen, resulting in an anion vibrational temperature of 200 K.

While the general appearance of the spectra as described above is consistent with the notion of a solvated $OH^-$ chromophore, the angular distributions of the photoelectrons can provide a more definitive confirmation of the structure. Rotation of the laser polarization with respect to the electron collection direction permitted determination of the photoelectron anisotropy parameter,[56–59] $\beta$, for each cluster size. The 351 nm photoelectron anisotropy parameter $\beta$ was measured to be $-0.67$, $-0.84$, $-0.77$, $-0.70$, and $-0.60$ for $OH^-(N_2O)_{n=1-5}$, respectively, and corresponds to electron ejection preferentially perpendicular to the laser polarization. This result compares with $\beta=-0.64$ for bare $OH^-$, and it is consistent with the earlier conclusion that the anionic core in the clusters is essentially $OH^-$.

The fact that vibrational structure is not resolved in the cluster ion spectra means that the usual spectroscopic identification of the origin transition (and hence the adiabatic electron affinity) is not possible. However, the VDE of an ion is well defined and can be measured to reasonable accuracy even in a featureless spectrum. While the EA corresponds to the minimum energy needed to remove an electron from the ground state of the anion, the VDE represents the energy required to remove an electron from the anion with the nuclei fixed at the equilibrium geometry of the anion. Thus, the VDE is readily determined from the binding energy corresponding to the maximum intensity in the photoelectron spectrum. The vertical detachment energies of each of the clusters are tabulated in Table I, along with the peak width [full width at half maximum (FWHM)].

In a complex where the equilibrium geometry of the anion is quite different from the equilibrium geometry of the neutral, photodetachment may produce a highly vibrationally excited neutral that is unstable with respect to dissociation,

TABLE I. Transition energies for $OH^-(N_2O)_n$ formed under liquid nitrogen cooled conditions.

| $OH(N_2O)_n$ | VDE (eV)[a] | FWHM (eV)[b] |
|---|---|---|
| $n=1$ | 2.189 | 0.100 |
| $n=2$ | 2.485 | 0.166 |
| $n=3$ | 2.761 | 0.167 |
| $n=4$ | 2.981 | 0.164 |
| $n=5$ | 3.146 | 0.150 |

[a]Vertical detachment energy.
[b]Full width at half maximum determined by fitting data to two Gaussians.

such as the case here. A more detailed description of each spectrum follows.

The spectrum of $OH^-(N_2O)$ shown in Fig. 2 is significantly broader ($\sim$100 meV) than that of bare $OH^-$ ($\sim$30 meV), even though the rotational broadening in the cluster will be much less than in the bare anion. Since the detached electron originates from the $OH^-$ chromophore, as in all the $OH^-/N_2O$ based clusters in this study, this broadened peak contains only the $OH^-(v''=0)\rightarrow OH(v'=0)$ transition for the chromophore. Thus the observed broadening in the cluster spectrum must be due to activation of unresolved van der Waals modes in the neutral and hot bands in the anion. The spectrum is also shifted $\sim$0.36 eV to higher VDE due to the large energy stabilization from the formation of the ion–neutral bond.

There must be a substantial contribution in the spectrum arising from low-frequency hot bands in $OH^-(N_2O)$; the importance of hot bands and additional information concerning the location of the origin transition can be obtained from varying the ion temperature and observing changes in the spectrum. The spectra of $OH^-(N_2O)$, obtained under both liquid nitrogen cooled and room-temperature ion source conditions, are shown in Fig. 3, scaled to the same peak intensity for comparison. The VDE of $OH^-(N_2O)$ at 300 K is 2.165 eV and the peak has a FWHM of 143 meV. Most of the spectral broadening when the ion temperature is raised to 300 K occurs on the low eBE side of the peak, which indicates activation of hot bands. We note that the VDE is temperature dependent, and decreases by 24 meV as the temperature is raised from 200 to 300 K.

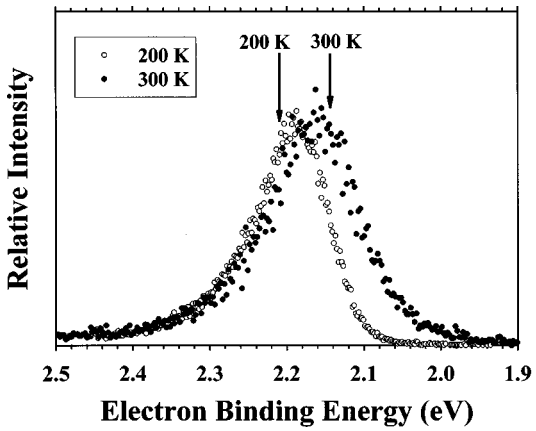


FIG. 3. Photoelectron spectra of $OH^-(N_2O)$ with anion vibrational temperatures of 200 (○) and 300 K (●).

The peak in the $OH^-(N_2O)_2$ spectrum is clearly broader than the corresponding feature in the spectrum of $OH^-(N_2O)$. The addition of another $N_2O$ solvent results in another ensemble of van der Waals modes that are activated upon photodetachment. Hence, this trend of wider peaks should continue with increasing solvation. The peak in the spectrum of $OH^-(N_2O)_3$ is wider, but the broadening is not as substantial as for the first two additions of solvent to the $OH^-$ chromophore. Eventually, of course, addition of an electron to an $OH(N_2O)_n$ cluster will make a very small change in geometry, and the photoelectron spectrum must become more narrow. A first guess might be to expect such behavior near the completion of the first solvent shell. In fact, beginning with $OH^-(N_2O)_4$, the peak widths do decrease as the number of solvent molecules increases. For all of the clusters reported here, the peak widths substantially exceed the estimated ion–neutral bond energy, $\sim$2 kcal/mol (80 meV) for $N_2O$ based complexes.[60,61] Thus, the peaks in all the spectra include contributions from transitions that result not only in electron detachment but also in dissociation of one or more $N_2O$ fragments in the neutral.

## IV. ANALYSIS AND DISCUSSION

In a system where the change in geometry is moderate, assigning an origin transition to obtain an EA is straightforward. Establishing an EA for a small cluster, however, is difficult because there is frequently a large geometry change between the anion and the neutral, as is the case with $OH^-(N_2O)_n$. In the following section, we show that there is significant intensity in the spectral origin of $OH^-(N_2O)$, despite the large change in geometry. This observation allows us to use spectra at two known ion temperatures to make a reasonably accurate determination of the adiabatic electron affinity of $OH(N_2O)$. With the value known, we then use a simple solvent model to obtain the adiabatic electron affinities of the larger clusters.

### A. $OH^-(N_2O)$

The electron affinity of $OH(N_2O)$ can be approximated using Eq. (1) to be 2.1 eV using 0.4 eV for $D_0[OH^-\cdots N_2O]$ from the *ab initio* calculations, and assuming $D_0[OH-N_2O]\approx D_0[HF-N_2O]=0.08$ eV, and the known EA(OH)=1.828 eV. This estimated position of the origin falls well within the observed photoelectron band in the spectrum, strongly suggesting that there is detectable signal at the adiabatic electron affinity. We can attempt to model the photoelectron spectrum using a standard Franck–Condon analysis procedure for a bound–bond transition, but the result is not definitive. Therefore, an alternate means of determining the origin position is required. The approach we have used takes advantage of our unique capability of measuring spectra at two different temperatures.

As seen in Fig. 3, the onset of the photoelectron band recedes significantly upon cooling the ions from 300 to 200

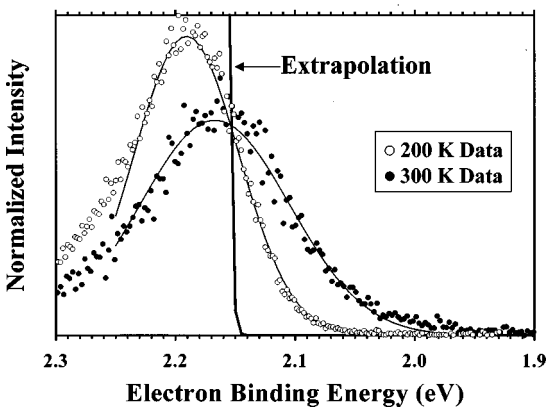


FIG. 4. The results of the extrapolation of the $OH^-(N_2O)$ spectra to 10 K vibrational temperature. The normalized data for the 200 and 300 K spectra are shown along with their fits to a single Gaussian. The crossing point of all three temperature models cross a single point whose location (2.15 eV) sets an upper limit for the EA of $OH(N_2O)$.

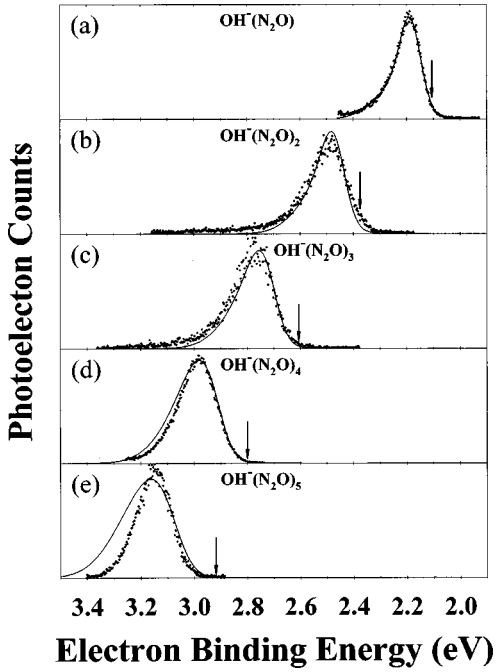


FIG. 5. Results of the convolution to model the spectrum of $OH^-(N_2O)_{n=2-5}$ from an empirical fit to the $OH^-(N_2O)$ spectrum [Fig. 5(a)]. Adiabatic electron affinities indicated by vertical arrows. Details are given in the text.

K. This is attributed to the quenching of hot bands as the vibrational temperature of the ions is lowered. Upon further cooling of the $OH^-(N_2O)$ ions below 200 K, the onset of the PES would be expected to recede to even higher eBE until the point near $T=0$ K, where the ion population will be fully cooled into the ground vibrational state. At this point, the onset of the spectrum will occur at the EA (provided there is significant intensity in the $0_0^0$ transition), as all the hot bands will be suppressed. With this in mind, we have carried out a temperature extrapolation of the data. For this analysis, the low energy portions of the 200 and 300 K spectra, which encompass the bound–bound transitions, are fit to Gaussian forms, then normalized. Assuming a Boltzmann relationship, the curves are then extrapolated to $T\approx 0$ K. The result for the extrapolation to $T=10$ K is shown in Fig. 4, along with the data at 200 and 300 K, and their fitted Gaussian curves. At 10 K, essentially all the ion population is cooled into the ground state, such that the onset should correspond to the EA. The extrapolated spectrum has an onset of 2.14 $\pm 0.02$ eV, in good agreement with the estimate provided above.

It should be noted that the normalized 200 and 300 K spectra cross at $\sim 2.15$ eV. Upon extrapolation to any temperature, the position of the curve at this crossing point does not change. Therefore, the crossing point is necessarily higher in energy than the EA and serves as an upper limit.

### B. $OH^-(N_2O)_{n=2-5}$

The numerous degrees of freedom in clusters prevent our examining the spectra $OH^-(N_2O)_{n=2-5}$ with our standard Franck–Condon analysis. Moreover, with additional solvent molecules, it is more difficult to locate the origin within the photoelectron band. In principle we could use the same sort of temperature extrapolation used for $OH^-(N_2O)$. However, the larger clusters are more difficult to prepare at warmer temperatures so that we are only able to make sufficient amounts for photoelectron studies at 200 K. More importantly, the temperature extrapolations may not be valid for the higher order clusters because it is not clear that there is significant intensity in the origin, a prerequisite for applying the temperature extrapolation. In this section we describe a simple approach for calculating the photoelectron spectra of the higher order clusters, and for approximating the location of the origin for each cluster. We first describe the procedure in detail for $OH^-(N_2O)_2$, and then provide results for the larger systems.

To model the spectra for $OH^-(N_2O)_2$, we use the shape of the photoelectron spectrum of $OH^-(N_2O)$ at 200 K as the Franck–Condon profile of a hydroxide core solvated by a single $N_2O$ molecule. For $OH^-(N_2O)_2$, we assume that the ion–solvent interactions are independent and similar to those in $OH^-(N_2O)$, so that photodetachment of larger clusters results in activation of several van der Waals modes in combination. Therefore, to calculate the spectrum of $OH^-(N_2O)_2$, we convolve the calculated spectrum of $OH^-(N_2O)$ with itself.

In order to simplify calculation, we first analytically describe the $OH^-(N_2O)$ spectrum as the sum of two Gaussians, $f(x)$ [Fig. 5(a)]. Then, to obtain the spectrum of $OH^-(N_2O)_2$ we convolute $f(x)$ with itself, representing the activation of two independent $N_2O$ motions, where $x=\mathrm{eBE}'-\mathrm{EA}$ [Eq. (3)],

$$G(\mathrm{eBE})=f(x)*f(\mathrm{eBE}-x)=\int_0^{\mathrm{eBE}} f(x)f(\mathrm{eBE}-x)dx. \tag{3}$$

The EA for the cluster is obtained by using the offset between the VDE and the origin determined from the calculated spectrum for that cluster. The result of the calculation,

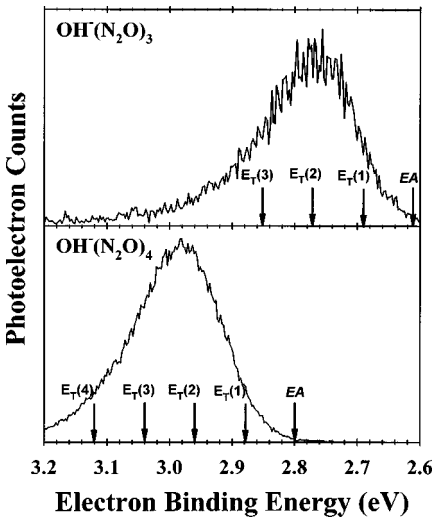


FIG. 6. Approximate locations of threshold $E_T(m)$ for loss of $m$ number of $N_2O$s upon photodetachment of $OH^-(N_2O)_3$ and $OH^-(N_2O)_4$.

shifted in energy to match the experimental VDE, is shown in Fig. 5(b), together with the experimental spectrum. Excellent agreement with the data is observed, indicating that this simple model does a reasonable job of describing the system.

For $OH^-(N_2O)_3$, the calculation involves convoluting the calculated $OH^-(N_2O)_2$ spectrum, $G(\mathrm{eBE})$ [Eq. (3)], with $f(x)$, which represents activation of yet another OH–$N_2O$ van der Waals mode. Thus, for $OH^-(N_2O)_3$ the shape of the spectral profile is calculated by Eq. (4),

$$H(\mathrm{eBE}) = f(x)^* G(\mathrm{eBE}-x) = \int_0^{\mathrm{eBE}} f(x) G(\mathrm{eBE}-x)\,dx. \tag{4}$$

The spectra of successively larger clusters are modeled in the same manner where the calculated $OH^-(N_2O)_{n-1}$ spectrum are convoluted with $f(x)$ to calculate the spectrum of $OH^-(N_2O)_n$. The calculations are compared with experiment in Fig. 5; the EA for each cluster is indicated by a vertical arrow. As expected, the intensity at the origin becomes successively weaker, and the EA shifts farther from the VDE as the size of the system increases.

For each cluster, we observe photoelectron signal at energies well above the energy required to dissociate one $N_2O$ from the neutral cluster. Therefore, as is the case for $OH^-(N_2O)$, photodetachment of $OH^-(N_2O)_{n=2-5}$ is likely to give products that are unstable with respect to dissociation. Moreover, for clusters where $n>1$, photodetachment can access multiple dissociation channels, resulting in ejection of $m$ $N_2O$ solvent molecules from the parent cluster [Eq. (5)],

$$OH^-(N_2O)_n + h\nu \rightarrow OH(N_2O)_{n-m} + mN_2O + e. \tag{5}$$

Having calculated the electron affinities and approximating $D_0[OH(N_2O)_{n-1}-N_2O] \approx 80$ meV in Eq. (1), the dissociation thresholds for loss of $N_2O$ molecules from the neutral clusters can be located. The electron affinities and the dissociative photodetachment thresholds for $OH^-(N_2O)_3$ and $OH^-(N_2O)_4$ are shown in Fig. 6, where $E_T(m)$ indicates a threshold for loss of $m$ number $N_2O$ solvents.

An important assumption of this model is that the Franck–Condon factors for each $N_2O$ molecule in a system are the same as those for the previous. The approximation will not be valid for large clusters, and it begins to fail for $OH^-(N_2O)_4$ and $OH^-(N_2O)_5$, where the width of the peaks *decreases* as the cluster grows larger. This indicates that addition of an electron begins to have less influence on the equilibrium geometry as the cluster grows larger. Hence, the nuclear displacements between the equilibrium structures of the anion and the neutral become smaller. This will also mean that the calculated electron affinities for these systems will be slightly lower than the actual electron affinities, and are thus lower limits for $OH(N_2O)_4$ and $OH(N_2O)_5$.

TABLE II. Electron affinities of $OH(N_2O)_{n=1-5}$ and bond dissociation energies of the corresponding anions.

| $OH^-(N_2O)_n$ | EA (eV) | $D_0(n,n-1)$[b] (eV) |
|---|---|---|
| $n=0$ | 1.828[a] | |
| $n=1$ | 2.12 | 0.37 |
| $n=2$ | 2.38 | 0.34 |
| $n=3$ | 2.60 | 0.30 |
| $n=4$ | $>2.80$ | $>0.28$ |
| $n=5$ | $>2.92$ | $>0.20$ |

[a]Ref. 19.

[b]Bond dissociation energy, $D_0[OH(N_2O)_{n-1}\cdots N_2O]$, given in Eq. (1) of text. For $OH^-(N_2O)_4$ and $OH^-(N_2O)_5$, the adiabatic binding energies (EA) and the corresponding bond dissociation energy [Eq. (1)] are given as lower limits. See text for details.

### C. Thermodynamics

In Table II, the calculated adiabatic electron affinities and the anion bond dissociation energies for loss of a single $N_2O$ as a function of cluster size $n[D_0(n, n-1)]$ are summarized. The neutral bond dissociation energy $D_0[OH(N_2O)_{n-1}-N_2O]$ is estimated to be 80 meV, similar to $D_0(HF-N_2O)$.[44,45]

The number of solvent molecules needed to complete the first solvent shell is dictated by the size of the chromophore, its binding energy to the solvent molecules, and the nature of the solvent. For $OH^-(N_2O)_n$, the anion bond dissociation energy steadily decreases as the cluster size increases by roughly the same amount upon stepwise solvation. No dramatic drop-off occurs in $D_0[OH^-(N_2O)_{n-1}-N_2O]$ to indicate that the first solvation shell has been completed. A full solvent shell for $I^-(N_2O)_n$, where the chromophore is larger, the solvent binding energy is smaller, and the solvent is identical, was determined to consist of 9 $N_2O$.[3] A larger chromophore would naturally require a larger shell to completely shield the charge. In a related study by Hiraoka *et al.*,[60] the first solvation shell in the $F^-(N_2O)_n$ is formed at $n=6$. The $F^-$ ion is roughly the same size as $OH^-$, and the $-\Delta H$ for $F^-(N_2O)$ is 9.87 kcal/mol (0.442 eV), compared to a bond dissociation energy for $OH^-(N_2O)$ of 0.37 eV. The stronger interaction in the $F^-/N_2O$ system suggests a smaller solute–solvent separation, indicating the possibility of a smaller solvation shell due to steric effects. From these comparisons to

$N_2O$ clusters solvating different chromophores, we expect that all the clusters in this study are within the first solvation shell.

## V. CONCLUSIONS

Negative-ion photoelectron spectroscopy of the $OH^-(N_2O)_{n=1-5}$ clusters has been used to study energetics in the anionic clusters and dissociation in the photodetachment process. The photoelectron spectra of $OH^-(N_2O)$ were taken at 200 and 300 K. An electron affinity was obtained for $OH(N_2O)$ using a simple temperature extrapolation. Despite the large geometry change in the equilibrium structures of the anion versus the neutral, significant Franck–Condon intensity exists in the $0_0^0$ transition.

Having located the origin for $OH^-(N_2O)$, the electron affinities of the higher order clusters, $OH^-(N_2O)_{n>1}$, are obtained through a convolution modeling, using the shape of the $OH^-(N_2O)$ spectrum. The model assumes that the binding energy in the neutral and displacements from the anion geometry are the same for larger clusters. The result is that addition of a $N_2O$ adds similar van der Waals modes to the previous $OH^-(N_2O)_{n-1}$ spectrum. Breakdown in the model begins to occur at $OH^-(N_2O)_4$, where the width of the spectrum begins to decrease as a function of cluster size. Thus, the displacement of the neutral from the anion geometry begins to decrease as the cluster becomes larger. This behavior may relate to the influence that the solvent–solvent interaction has on the structure of the anion as the size of the cluster approaches the closing of the first solvation shell. As the cluster size increases, solvent–solvent interaction exerts a greater influence on the structure of the cluster as opposed to the smaller clusters ($n<4$) where the structure is dominated by the solute–solvent (ion–neutral) interaction.

From the results of the modeling, adiabatic electron affinities of $OH(N_2O)_{n>1}$ are obtained, as well as bond dissociation energies in the anions. It is apparent from the locations of the origin and the width of the spectrum that photodetachment accesses dissociation channels corresponding to loss of multiple $N_2O$ molecules.

## ACKNOWLEDGMENTS

We thank Professor John C. Sheldon for providing his unpublished results on the $OH^- + N_2O$ potential energy surface. This work has been supported by National Science Foundation Grant Nos. CHE97-03486 and PHY95-12150, and the Air Force Office of Scientific Research AASERT Program.

[1] S. T. Arnold, J. H. Hendricks, and K. H. Bowen, J. Chem. Phys. **102**, 39 (1995).
[2] D. W. Arnold, S. E. Bradforth, E. H. Kim, and D. M. Neumark, J. Chem. Phys. **102**, 3493 (1995).
[3] D. W. Arnold, S. E. Bradforth, E. H. Kim, and D. M. Neumark, J. Chem. Phys. **102**, 3510 (1995).
[4] D. M. Cyr, M. G. Scarton, and M. A. Johnson, J. Chem. Phys. **99**, 4869 (1993).
[5] J. V. Coe, J. T. Snodgrass, K. M. Friedhoff, and K. H. Bowen, J. Chem. Phys. **87**, 4302 (1987).
[6] G. Markovich, S. Pollack, R. Giniger, and O. Cheshnovsky, J. Chem. Phys. **101**, 9344 (1994).
[7] L. A. Posey and M. A. Johnson, J. Chem. Phys. **88**, 5383 (1988).
[8] J. Ho, K. M. Ervin, and W. C. Lineberger, J. Chem. Phys. **93**, 6987 (1990).
[9] D. G. Leopold, J. Ho, and W. C. Lineberger, J. Chem. Phys. **86**, 1715 (1987).
[10] J. V. Coe, G. H. Lee, J. G. Eaton, S. T. Arnold, H. W. Sarkas, K. H. Bowen, C. Ludewigt, and H. Haberland, J. Chem. Phys. **92**, 3980 (1990).
[11] H. W. Sarkas, L. H. Kidder, and K. H. Bowen, J. Chem. Phys. **102**, 57 (1995).
[12] M. J. DeLuca, B. Niu, and M. A. Johnson, J. Chem. Phys. **88**, 5857 (1988).
[13] D. W. Arnold, S. E. Bradforth, T. N. Kitsopoulos, and D. M. Neumark, J. Chem. Phys. **95**, 8753 (1991).
[14] O. Cheshnovsky, S. H. Yang, C. L. Pettiette, M. J. Craycraft, Y. Liu, and R. E. Smalley, Chem. Phys. Lett. **138**, 119 (1987).
[15] O. Cheshnovsky, K. J. Taylor, J. Conceicao, and R. E. Smalley, Phys. Rev. Lett. **64**, 1785 (1990).
[16] H. Kietzmann, J. Morenzin, P. S. Bechthold, G. Gantefor, W. Eberhardt, D. S. Yang, P. A. Hackett, R. Fournier, T. Pang, and C. F. Chen, Phys. Rev. Lett. **77**, 4528 (1996).
[17] G. Gantefor, H. Handschuh, H. Moller, C. Y. Cha, P. S. Bechthold, and W. Eberhardt, Surf. Rev. Lett. **3**, 399 (1996).
[18] G. Gantefor, S. Hunsicker, and R. O. Jones, Chem. Phys. Lett. **0236**, 43 (1995).
[19] M. Gausa, R. Kaschner, H. O. Lutz, G. Seifert, and K. H. Meiwesbroer, Chem. Phys. Lett. **230**, 99 (1994).
[20] M. Gausa, R. Kaschner, G. Seifert, J. H. Faehrmann, H. O. Lutz, and K. H. Meiwesbroer, J. Chem. Phys. **104**, 9719 (1996).
[21] A. Nakajima, H. Kawamata, T. Hayase, Y. Negishi, and K. Kaya, Z. Phys. D **40**, 17 (1997).
[22] Y. Negishi, H. Kawamata, T. Hayase, M. Gomei, R. Kishi, F. Hayakawa, A. Nakajima, and K. Kaya, Chem. Phys. Lett. **269**, 199 (1997).
[23] K. Kaya, H. Kawamata, Y. Negishi, T. Hayase, R. Kishi, and A. Nakajima, Z. Phys. D **40**, 5 (1997).
[24] H. B. Wu, S. R. Desai, and L. S. Wang, Phys. Rev. Lett. **77**, 2436 (1996).
[25] H. B. Wu, S. R. Desai, and L. S. Wang, Phys. Rev. Lett. **76**, 212 (1996).
[26] L. S. Wang, H. B. Wu, and H. S. Cheng, Phys. Rev. B **55**, 12884 (1997).
[27] J. Conceicao, R. T. Laaksonen, L. S. Wang, T. Guo, P. Nordlander, and R. E. Smalley, Phys. Rev. B **51**, 4668 (1995).
[28] L. S. Wang, H. S. Cheng, and J. W. Fan, J. Chem. Phys. **102**, 9480 (1995).
[29] C. R. Sherwood, M. C. Garner, K. A. Hanold, K. M. Strong, and R. E. Continetti, J. Chem. Phys. **102**, 6949 (1995).
[30] M. Meot-Ner and L. W. Sieck, J. Phys. Chem. **90**, 6687 (1986).
[31] J. C. Paul and P. Kebarle, J. Phys. Chem. **94**, 5184 (1990).
[32] E. Debeer, E. H. Kim, D. M. Neumark, R. F. Gunion, and W. C. Lineberger, J. Phys. Chem. **99**, 13627 (1995).
[33] D. W. Arnold, X. Cangshan, and D. M. Neumark, J. Chem. Phys. **102**, 6088 (1995).
[34] W. H. Thompson, H. O. Karlsson, and W. H. Miller, J. Chem. Phys. **105**, 5387 (1996).
[35] D. C. Clary, J. Gregory, M. J. T. Jordan, and E. Kauppi, J. Chem. Soc. Faraday Trans. **93**, 747 (1997).
[36] D. Wang, J. Z. H. Zhang, and C.-H. Yu, Chem. Phys. Lett. **273**, 171 (1997).
[37] P. Frey, M. Lawlen, F. Breyer, H. Klar, and H. Hotop, Z. Phys. A **304**, 155 (1982).
[38] J. J. Grabowski, Ph.D. thesis, University of Colorado, 1983, pp. 190–221.
[39] V. M. Bierbaum, J. J. Grabowski, and C. H. DePuy, J. Phys. Chem. **88**, 1389 (1984).
[40] S. E. Barlow and V. M. Bierbaum, J. Chem. Phys. **92**, 3442 (1990).
[41] J. C. Sheldon (unpublished results).
[42] L. H. Sharpen, J. S. Muenter, and V. W. Laurie, J. Chem. Phys. **53**, 2513 (1970).
[43] A. D. Buckingham, C. Graham, and J. H. Williams, Mol. Phys. **49**, 703 (1983).
[44] K. Mogi, T. Komine, and K. Hirao, J. Chem. Phys. **95**, 8999 (1991).
[45] C. M. Lovejoy and D. J. Nesbitt, J. Chem. Phys. **90**, 4671 (1989).
[46] Y. P. Zeng, S. W. Sharpe, D. Reifschneider, C. Wittig, and R. A. Beaudet, J. Chem. Phys. **93**, 183 (1990).

[47] The open-shell site on OH should not affect the structure of the van der Waals complex.
[48] K. M. Ervin and W. C. Lineberger, in *Advances in Gas Phase Ion Chemistry*, edited by N. G. Adams and L. M. Babcock (JAI, Greenwich, 1992), Vol. 1, p. 121.
[49] K. M. Ervin, J. Ho, and W. C. Lineberger, J. Chem. Phys. **91**, 5974 (1989).
[50] D. M. Neumark, K. R. Lykke, T. Andersen, and W. C. Lineberger, Phys. Rev. A **32**, 1890 (1985).
[51] P. G. Wenthold, M. L. Polak, and W. C. Lineberger, J. Phys. Chem. **100**, 6920 (1996).
[52] P. A. Schulz, R. D. Mead, P. L. Jones, and W. C. Lineberger, J. Chem. Phys. **77**, 1153 (1982).
[53] H. Hotop, T. A. Patterson, and W. C. Lineberger, J. Chem. Phys. **60**, 1806 (1974).
[54] J. R. Smith, J. B. Kim, and W. C. Lineberger, Phys. Rev. A **55**, 2036 (1997).
[55] K. P. Huber and G. Herzberg, *Constants of Diatomic Molecules* (Van Nostrand Reinhold, New York, 1979).
[56] J. Cooper and R. N. Zare, J. Chem. Phys. **48**, 942 (1968).
[57] J. Cooper and R. N. Zare, J. Chem. Phys. **49**, 4252 (1968).
[58] J. L. Hall and M. W. Siegel, J. Chem. Phys. **48**, 943 (1968).
[59] D. Hanstorp, C. Bengtsson, and D. J. Larson, Phys. Rev. A **40**, 670 (1989).
[60] K. Hiraoka, K. Aruga, S. Fujimaki, and S. Yamabe, J. Am. Soc. Mass Spectrom. **4**, 58 (1993).
[61] K. Hiraoka, S. Fujimaki, K. Aruga, and S. Yamabe, J. Phys. Chem. **98**, 8295 (1994).